

Metamaterial-Based Flat Lens: Wave Concept Iterative Process Approach

Mohamed K. Azizi^{1, *}, Henri Baudrand², Lassaad Latrach¹, and Ali Gharsallah¹

Abstract—Metamaterials left-hand negative refractive index has remarkable optical properties; this paper presents the results obtained from the study of a flat metamaterial lens. Particular interest is given to the interaction of electromagnetic waves with metamaterials in the structure of the lens Pendry. Using the new approach of the Wave Concept Iterative Process (WCIP) based on the auxiliary sources helps to visualize the behavior of the electric field in the metamaterial band and outside of its interfaces. The simulation results show an amplification of evanescent waves in the metamaterials with an index of $n = -1$, which corresponds to a resonance phenomenon to which the attenuation solution is canceled, leaving only the actual growth of these waves. This amplification permits the reconstruction of the image of the source with a higher resolution.

1. INTRODUCTION

The way of negative refraction has sparked a rare craze after passionate debate generated by controversies on electromagnetic models. In 1968, the Russian Victor Veselago invented the converging lens plate [1]. In the late 1990s, Pendry and his team carried out work on metal wire networks (“wire medium”) [2, 3] and (split-ring resonators or SRR) [4]. Given the difficulty to achieve super-lenses, teams of researchers developed other systems exploiting the characteristics of metamaterials to achieve a sub-wave length resolution. These new devices include the wireless networks [5, 6] operating in the pipeline system, networks of nanoparticles [7], and the hyper-lenses using structures of spherical and anisotropic form [8–10]. Pendry later studied the flat lens with a refractive index $n = -1$, and that is how we got an almost unlimited power of resolution. Unlike the flat lens Veselago [11], the annular lens (1994) proposed a new fact described as “homeopathic.” The perfect lens Pendry [12] can lead to a theoretically unlimited resolution, thanks to the amplification of evanescent waves, which allow light to play the ‘pass-wall’, and this looks like the photon sieve of Thomas Ebbesen, who relied on the existence of spoof plasmons [13]. At first, a convex lens whose refractive index is higher than that of the vacuum produces an upside-down image of an object in which the details that are smaller than a half wavelength are not resolved. This barrier once thought insurmountable before the concept of the perfect lens is the equivalence of the Heisenberg inequality in quantum mechanics. Pendry discovered that metals as the cornerstone of metamaterials [14] are highly absorbent to optical wavelengths, which limits the resolution of the super lens by Pendry.

In 2005, a Los Angeles college team experimentally demonstrated a resolution higher than fifth wavelength through a metamaterial [15] consisting of a thin silver film sandwiched between two semiconductor layers for a frequency in the visible spectrum [16]. Since then, the realization of super lenses rat race has begun [17], with resolutions up today twentieth wavelength in the near infrared. The realization of such a component for optical represents a technological challenge, besides that this

Received 7 March 2017, Accepted 27 May 2017, Scheduled 6 June 2017

* Corresponding author: Mohamed Karim Azizi (Medkarim.azizi@gmail.com).

¹ Unit of research Circuits and Electronics Systems High Frequency, Faculty of Science, University El Manar, Tunis, Tunisia. ² Laplace Lab, Department of Electronics, Faculty ENSEEIHT, University of Toulouse, France.

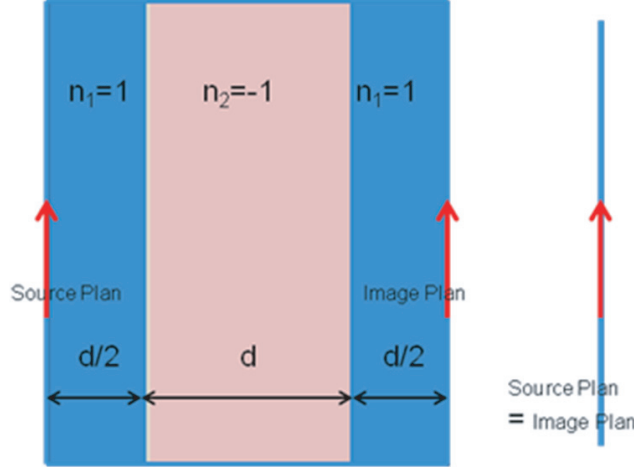


Figure 1. Veselago flat lens: The metamaterial lens of width d and refractive index $n_2 = -1$ is surrounded by air ($n_1 = 1$). The width d is chosen such as le distance between source plan and first metmaterial plan is equal to $d/2$.

lens allows another form of invisibility to be considered [18]. The negative index of refraction is due to negative values of both the permittivity ϵ and permeability μ . Through Veselago flat lens, images are merged with their source in the virtual space. This allows us to conclude that anything in the proximity of the lens should be virtually invisible as it is reduced to one line (Fig. 1) in physical space.

All these studies have helped to have an image with higher resolution, but not a perfect image.

In this paper, we will study the flat lens and try to improve the image resolution using a new approach to iterative WCIP further amplifying the evanescent waves, and the restoration of evanescent waves in the image plane provides a very high-resolution image. The first part of this paper will be dedicated to the presentation of the new approach to iterative WCIP that involves the study of a single unit cell of the structure. In the second part of this paper, we will study the structure of the lens flat formed by metamaterial cells by determining the field distribution over the entire structure in order to see and discuss the resolution of the image of the source. The last part of this paper is devoted to the interpretation of the simulation results and the improvement in the resolution by adjusting the amplification of evanescent waves. Given the lack of accuracy, the simulation is impossible with equivalent environment, even the conventional methods (EF, FDTD) does not give good results. Taking a cell with localized elements is original and can solve this problem, based especially on the equation in the spectral domain.

2. FLAT LENS MADE FROM METAMATERIALS

2.1. New Approach to WCIP Method

The concept of wave is introduced by expressing the incidental and reflected waves into the interface according to the electromagnetic sizes, the electric field and the density of current tangential on the surface Ω . These waves are expressed by:

$$A = \frac{1}{2\sqrt{Z_0}}(E + Z_0 J) \quad (1)$$

$$B = \frac{1}{2\sqrt{Z_0}}(E - Z_0 J) \quad (2)$$

For the total structure, the principle of WCIP is characterized by two operators linking the incident and reflected waves by:

$$A = SB + A_0 \quad (3)$$

$$B = \Gamma A \quad (4)$$

S : the diffraction operator is expressed in the spatial domain.
 Γ : the operator of reflection is expressed in the frequency domain.
 A_0 : the excitation waves.

Once Γ and S -parameters are determined for the whole structure, we can apply the iterative process. The WCIP is applied in the case where the pixels are homogeneous, usually metal or dielectric for application to planar circuits. We will treat the case where the pixels are themselves devices that can be complex to model almost-periodic structures.

The theory of the new approach of iterative WCIP method for almost periodic structures is described in the article [19].

2.2. Elementary Cell

We isolate the elementary cell (Fig. 2) of the two-dimensional structure to calculate the values of the permittivity and the corresponding permeability.

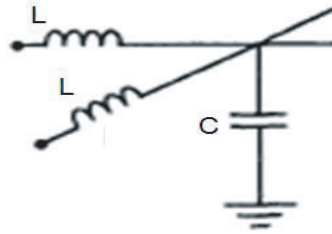


Figure 2. Unit cell composed of two inductors (l) and a capacity (C).

The elementary cell used is formed by inductors and capacity. The values of L and C determine the values of μ and ε , and we can write the index this way:

$$n = \sqrt{\frac{\varepsilon}{\varepsilon_r}} = \sqrt{\varepsilon_r} \quad (5)$$

δl is the length of the unit cell, and the capacitance per unit length is equal to:

$$C = C_0/\delta l \quad (6)$$

$$L = L_0/\delta l. \quad (7)$$

$c = 3.108 \text{ m/s}$ is the light velocity, and C_0 and L_0 are the values that give $n = 1$. Suppose that the impedance of the line is equal to 120π , (I and V represent E and J). With $\varepsilon_r = 1$, we find $n = 1$.

In the following, we will set L to L_0 , and C may change. With the index n , we obtain

$$C = C_0 n^2 \quad (8)$$

2.3. The Flat Metamaterial Lens

In conventional imaging that uses lenses, the resolution limit will be imposed. This diffraction limit is attributed to the wavelength of electromagnetic waves. By introducing evanescent waves Pendry developed a new analysis of the lens Veselago (Fig. 2) and observed that these lenses could overcome the diffraction limit [20].

The lens Veselago (Figure 3) would provide a perfect image if its refractive index $n = -1$. The left-hand lens realizes an image with a super-resolution focusing on amplification and restoration of evanescent waves. This restoration of evanescent waves in the image plane provides a very high resolution image. The physical mechanism behind the growth of the evanescent wave is very interesting since index $n = -1$ corresponds to a resonance phenomenon wherein the attenuation solution is canceled, leaving only the actual growth of these evanescent waves.

Figure 4 presents a flat version of the lens Veselago which was built at the University of Toronto [21]. The lens is a gate structure composed of 5×19 cells strips, containing series of capacitor (C_0) and short-circuited with an inductance (L_0). This structure NRI is sandwiched between two printed discharged

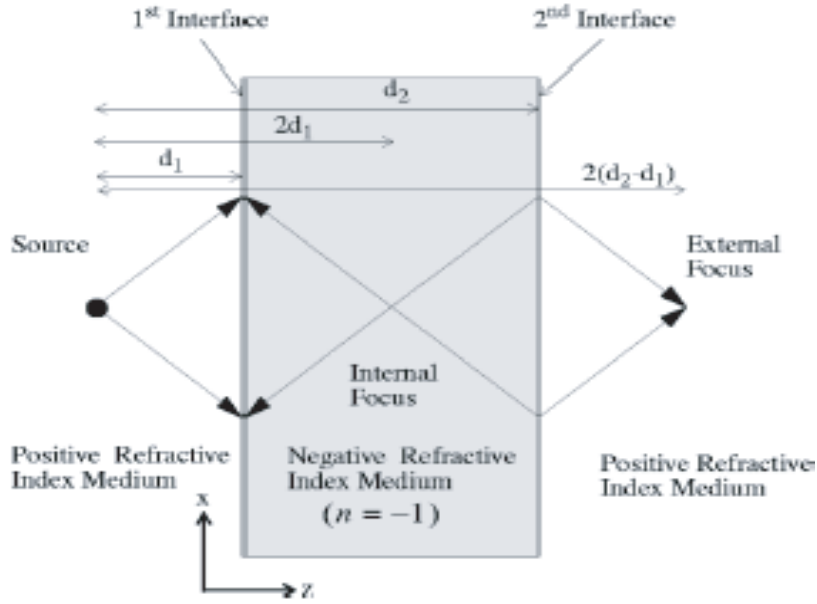


Figure 3. Metamaterial lens: Schematic representation of the positions of the source and the formed image relatively to the input and output interface of the lens.

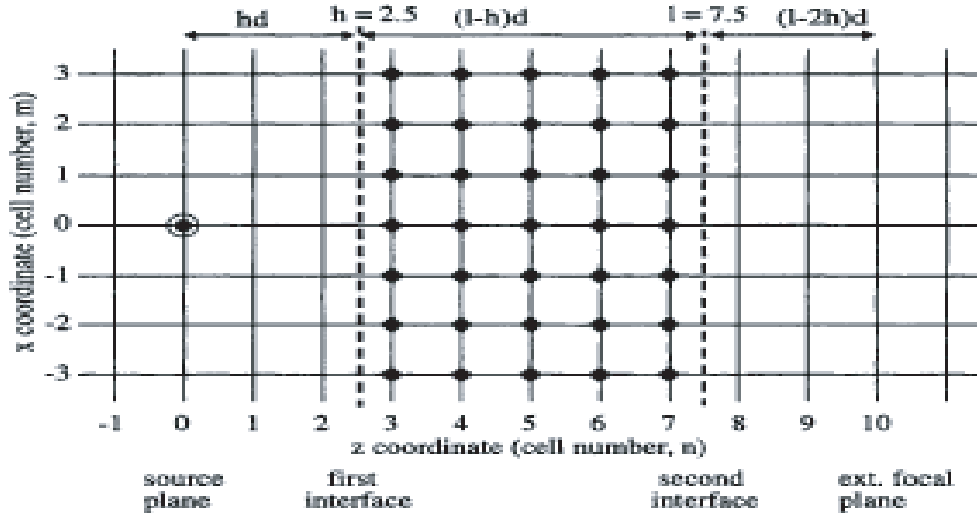


Figure 4. Structure of Lens Veselago: Two cell-columns separate the source from the lens first interface. The metamaterial lens is formed of 5 column of matemateriel cells.

grids that act as homogeneous media having a positive refractive index. The first unloaded network is excited with a point source attached to the left grid, which is reproduced by the NRI lens at the second gate. We want to determine the distribution of the electric field.

The unit cell is shown in (Fig. 5) formed of three sources and two resistances (r). The sources $E1$, $E3$ and $E5$ are based on electrical walls to have a current, i.e., if they are based on magnetic walls or periodic current, the current is zero.

There are 8 equations with 8 unknowns

$$V_2 = V_4 = E_5 \quad (9)$$

$$I_1 + I_2 + I_3 + I_4 + I_5 = 0 \quad (10)$$

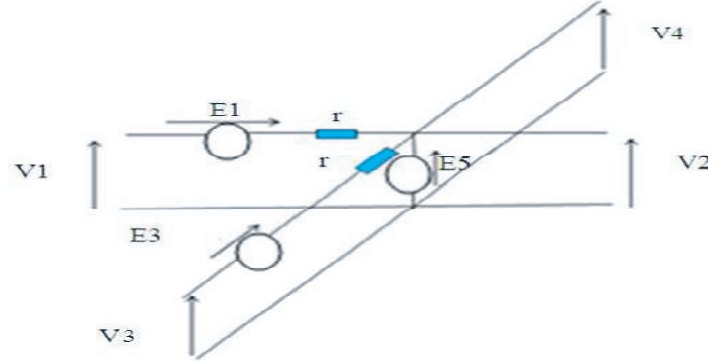


Figure 5. Unit cell formed of three sources and two resistances (r).

$$V_1 + E_1 - rI_1 - E_5 = 0 \tag{11}$$

$$V_3 + E_3 - rI_3 - E_5 = 0 \tag{12}$$

$$r \begin{vmatrix} I_1 \\ I_3 \\ I_5 \end{vmatrix} = \begin{vmatrix} 1 & 0 & a \\ 0 & 1 & b \\ a^* & b^* & |a|^2 + |b|^2 \end{vmatrix} \begin{vmatrix} E_1 \\ E_3 \\ E_5 \end{vmatrix} \tag{13}$$

We suppose that

$$a = e^{-j\alpha}(1 - e^{j\alpha})$$

$$b = e^{-j\beta}(1 - e^{j\beta})$$

We must now calculate the specific values in order to determine the reflection coefficient.

Now we search the admittance matrix:

$$\bar{\bar{Y}} = \frac{1}{r} (YY^+ + (1 + |a|^2 + |b|^2) ZZ^+) \tag{14}$$

$$\Gamma = \frac{1 - Z_0\bar{\bar{Y}}}{1 + Z_0\bar{\bar{Y}}} \tag{15}$$

with Z_0 : impedance

$$\left(1 + \frac{Z_0}{r} (YY^+ + (1 + |a|^2 + |b|^2) ZZ^+) \right)^{-1} = 1 + \alpha YY^+ + \beta ZZ^+ \tag{16}$$

$$\Gamma = 1 - 2YY^+ - 2ZZ^+ \tag{17}$$

3. NUMERICAL RESULTS AND DISCUSSION

In order to simulate the structure (Fig. 6), we placed a source cell at the third line at a distance from the first interface of the metamaterial order $d1 = 2d$ (or corresponding to two cell lines), and the second interface [22] is located at a distance of $2d$ from the first interface. The source image is focused at a distance of $2d$ behind the second interface to validate this study [23].

We observe (in Fig. 7) evanescent waves growing in the NRI-TL lens. The dotted lines indicate the location of the NRI region, and the solid lines represent the location of the source (left) and the external image (right). The structure size is 36×36 , and the cell length is $\lambda/36$. For metamaterial, we used a permittivity $\epsilon = -1$ and permeability $\mu = -1$. Thus, we have an optical device likely to achieve a perfect image [24] of an object without limitation due to diffraction. Due to negative refraction, we can see perfect images, as long as the period of the material is sufficiently small compared to the wavelength (Fig. 8). The abolition of the boundary due to the diffraction comes from the amplification of evanescent waves. This amplification, which comes from the sign inversion of the wave vector, allows the evanescent

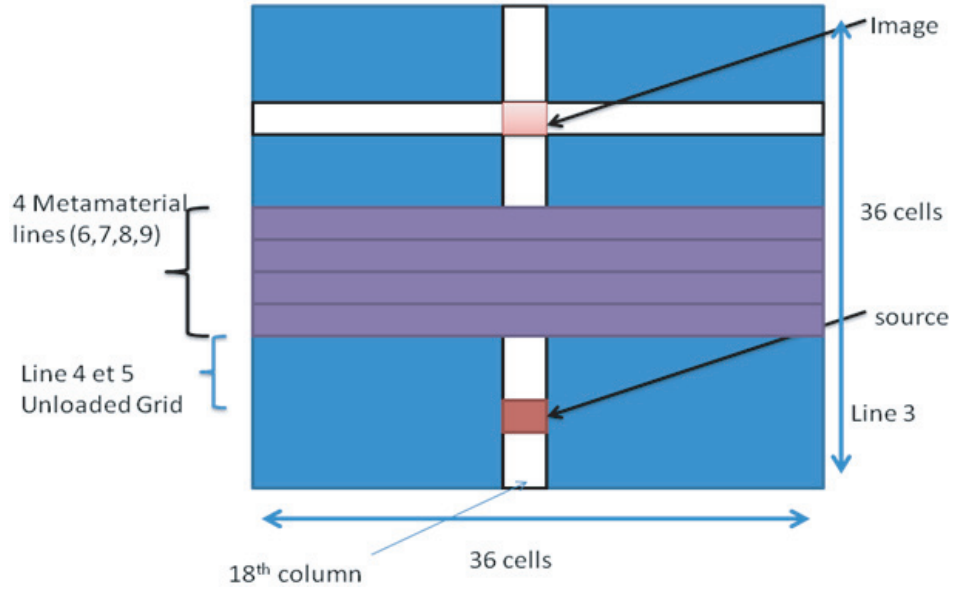


Figure 6. Structure of the lens (36 columns and 36 rows of cells). The source is placed at the 18th cell of this row. The metamaterial cells compose the rows 6 to 9.

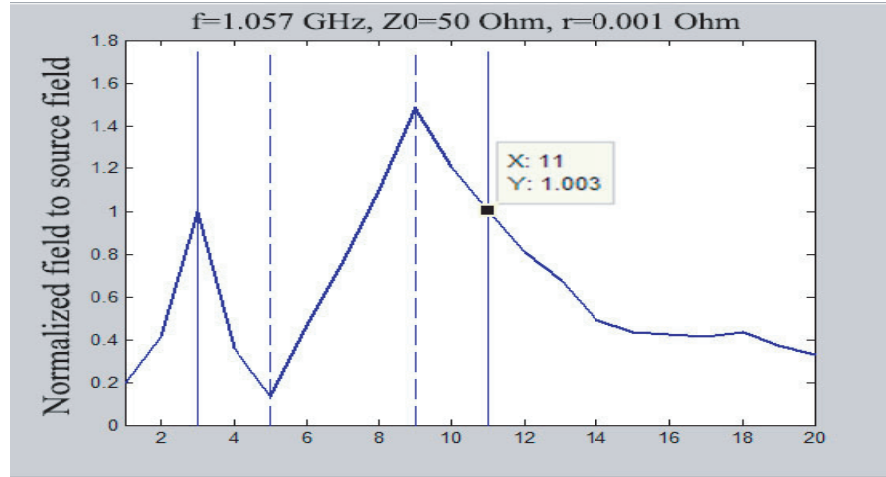


Figure 7. Behavioral fields $|Ez|$ along the cells of the 18th column. The field amplitude at the source is 1 and reach the value 1.42 in the metamaterial region. The image field amplitude (11th cell of this row) is equal to the source one.

wave to be transmitted to the image without attenuation [25]. To achieve this, it is necessary that the transmission is done without reflection at interfaces with the classic external environment. If it is air or vacuum, with $\varepsilon_r = \mu_r = 1$, it is necessary that the left-hand material has $\varepsilon_r = -1$ and $\mu_r = -1$.

We changed the structure while keeping the same number of pixels between the source and the first interface of the lens. Also, we kept the number of pixels forming the thickness of the lens. An improvement was made to the result of the field by amplifying the evanescent waves and gives us a better resolution of the image by acting on the following parameters: Normal cell: $L = 18e - 9H$; $C = 3.2e - 13F$, $n = 1.1269$. metamaterial Cell: $n_{meta} = -1 \times n = -1.269$.

Frequency = 1.057 GHz, $Z_0 = 120 * \pi$, Cell length: $dl = 0.06735$ mm.

The following figure (Fig. 9) shows the behavior of the field Ez over all the structure. We show

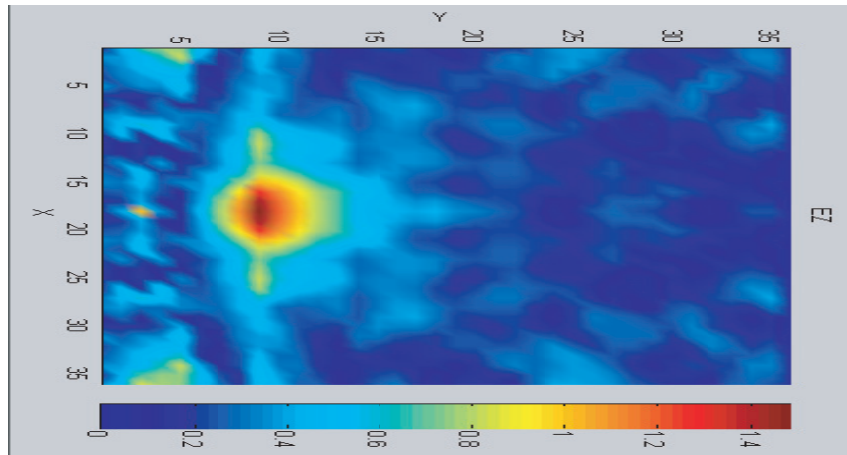


Figure 8. Mapping of the fields $|Ez|$ over the studied structure.

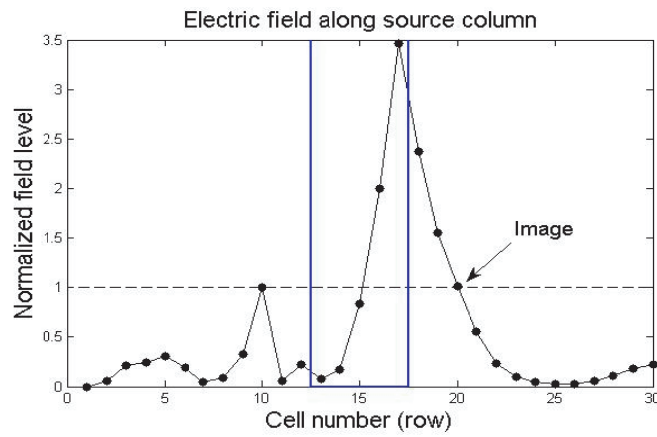


Figure 9. Behavioral fields $|Ez|$ along the column containing the source cell. The field amplitude at the source is 1 and reach the value 3.5 in the metamaterial region. The image field amplitude is equal to the source one.

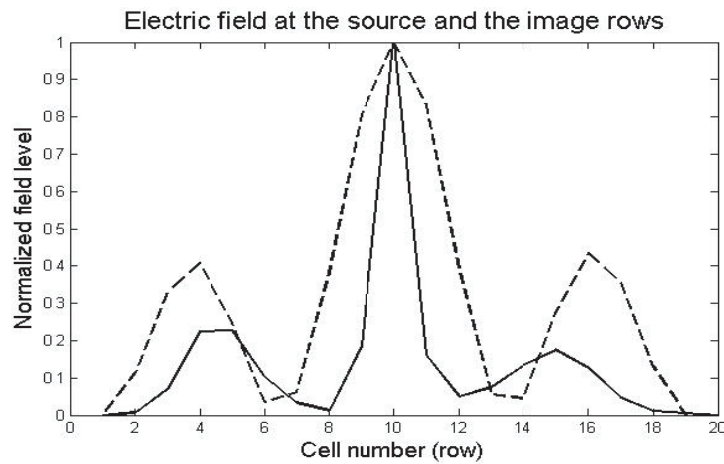


Figure 10. The normalized electric field along the cells composing the rows containing the source (continuous line) and the formed image (dashed line).

in (Fig. 10) the normalized vertical electric field at the source ($n = 0$) and the external focal plane ($n = 10$) at 1.057 GHz along with the theoretical diffraction-limited images (linear scale).

4. CONCLUSION

This article presents the application of a new approach to WCIP method based on two circuits in almost periodic dimensions for optical devices such as superlenses. This new approach has been used to study flat lens composed of metamaterial-based cells. Our results show that the distribution of the field over the flat lens is significantly amplified by the evanescent waves in the metamaterial cells. The studied structure allowed an improvement of the source-image resolution.

REFERENCES

1. Veselago, V., "Electrodynamics of substances with simultaneously negative electrical and magnetic permeabilities," *Sov. Phys. Usp.*, Vol. 10, No. 4, 509–514, 1968.
2. Pendry, J., A. Holden, W. Stewart, and I. Youngs, "Extremely low frequency plasmons in metallic mesostructures," *Physical Review Letters*, Vol. 76, No. 25, 4773–4776, 1996.
3. Pendry, J., A. Holden, D. Robbins, and W. Stewart, "Low frequency plasmons in thin-wire structures," *Journal of Physics: Condensed Matter*, Vol. 10, 4785, 1998.
4. Pendry, J., A. Holden, D. Robbins, and W. Stewart, "Magnetism from conductors and enhanced nonlinear phenomena," *IEEE Transactions on Microwave Theory and Techniques*, Vol. 47, No. 11, 2075–2084, 1999.
5. Belov, P. A., C. R. Simovski, and P. Ikonen, "Canalization of subwavelength images by electromagnetic crystals," *Phys. Rev. B*, Vol. 71, 193105, May 2005.
6. Belov, P. A. and M. G. Silveirinha, "Resolution of subwavelength transmission devices formed by a wire medium," *Phys. Rev. E*, Vol. 73, 056607, May 2006.
7. Simovski, C. R., A. J. Viitanen, and S. A. Tretyakov, "Resonator mode in chains of silver spheres and its possible application," *Phys. Rev. E*, Vol. 72, 066606, Dec. 2005.
8. Salandrino, A. and N. Engheta, "Far-field subdiffraction optical microscopy using metamaterial crystals: Theory and simulations," *Phys. Rev. B*, Vol. 74, 075103, Aug. 2006.
9. Jacob, Z., L. V. Alekseyev, and E. Narimanov, "Optical hyperlens: Far-field imaging beyond the diffraction limit," *Optics Express*, Vol. 14, No. 18, 8247–8256, 2006.
10. Liu, Z., H. Lee, Y. Xiong, C. Sun, and X. Zhang, "Far-field optical hyperlens magnifying sub-diffraction-limited objects," *Science*, Vol. 315, 1686, Mar. 2007.
11. Veselago, V. G., "The electrodynamics of substances with simultaneously negative values of ϵ and μ ," *Sov. Phys. Usp.*, Vol. 10, No. 4, 509–514, Jan. 1967.
12. Pendry, J. B., "Negative refraction makes a perfect lens," *Phys. Rev. Lett.*, Vol. 85, No. 18, 3966–3969, Oct. 2000.
13. Anantha Ramakrishna, S., et al., "Plasmonic interaction of visible light with gold nanoscale checkerboards," *Physical Review B*, Vol. 84, 245424, 2011.
14. Iyer, A. K. and G. V. Eleftheriades, "Negative refractive index metamaterials supporting 2-D waves," *IEEE MTT-S International Microwave Symposium Digest*, Vol. 2, 1067–1070, Seattle, WA, Jun. 2–7, 2002.
15. Naoui, S., L. Latrach, and A. Gharsallah, "Metamaterials dipole antenna by using split ring resonators for RFID technology," *Wiley Microwave Optical Technology Letters*, Vol. 56, 2899–2903, 2014, DOI 10.1002/mop.28731.
16. Guenneau, S. and B. Gralak, "Une optique classique sens dessus dessous," *Les Dossiers De La Recherche*, Vol. 38, 32, 2010.
17. Liu, Z., H. Lee, Y. Xiong, C. Sun, and X. Zhang, "Far-field optical hyperlens magnifying sub-diffraction-limited objects," *Science*, Vol. 315, 1686, Mar. 2007.
18. Guenneau, S., et al., "The colors of cloaks," *Journal of Optics*, Vol. 13, 024014, 2011.

19. Azizi, M. K., L. Latrach, N. Raveu, A. Gharsallah, and H. Baudrand, "A new approach of almost periodic lumped elements circuits by an iterative method using auxiliary sources," *American Journal of Applied Sciences*, Vol. 10, No. 11, 1457–1472, 2013, ISSN: 1546-9239.
20. Pendry, J. B., A. J. Holden, D. J. Robbins, and W. J. Stewart, "Magnetism from conductors and enhanced nonlinear phenomena," *IEEE Transactions on Microwave Theory and Techniques*, Vol. 47, No. 11, 2075–2084, Nov. 1999.
21. Iyer, A. K. and G. V. Eleftheriades, "Negative refractive index metamaterials supporting 2-D waves," *IEEE MTT-S International Microwave Symposium Digest*, Vol. 2, 1067–1070, Seattle, WA, Jun. 2–7, 2002.
22. Pendry, J. B., "Negative refraction makes a perfect lens," *Phys. Rev. Lett.*, Vol. 85, No. 18, 3966–3969, Oct. 2000.
23. Iyer, A. K., P. C. Kremer, and G. V. Eleftheriades, "Experimental and theoretical verification of focusing in a large, periodically loaded transmission line negative refractive index metamaterial," *Opt. Express*, Vol. 11, 696–708, Apr. 2003.
24. Iyer, A. K., A. Grbic, and G. V. Eleftheriades, "Sub-wavelength focusing in loaded transmission line negative refractive index metamaterials," *IEEE MTT-S International Microwave Symposium Digest*, 199–202, Philadelphia, PA, Jun. 8–13, 2003.
25. Azizi, M. K., H. Baudrand, T. Elbellili, and A. Gharsallah, "Almost periodic lumped elements structure modeling using iterative method: Application to photonic jets and planar lenses," *Progress In Electromagnetics Research M*, Vol. 55, 121–132, 2017.